SANDIA REPORT
SAND2005-0366
Unlimited Release
Printed January 2005

Final LDRD Report: Design and Fabriction of Advanced Device Structures for Ultra High Efficiency Solid State Lighting

Arthur J. Fischer, Mary H. Crawford, Daniel D. Koleske, Andrew A. Allerman, Katherine H. A. Bogart, Joel R. Wendt, and Randy J. Shull

Prepared by
Sandia National Laboratories
Albuquerque, New Mexico 87185 and Livermore, California 94550

Sandia is a multiprogram laboratory operated by Sandia Corporation,

a Lockheed Martin Company, for the United States Department of Energy's
National Nuclear Security Administration under Contract DE-AC04-94AL85000.

Sandia National Laboratories

Issued by Sandia National Laboratories, operated for the United States Department of Energy by Sandia Corporation.

Printed in the United States of America. This report has been reproduced directly from the best available copy.

Available to DOE and DOE contractors from
U.S. Department of Energy
Office of Scientific and Technical Information
P.O. Box 62
Oak Ridge, TN 37831

Telephone: (865)576-8401
Facsimile: (865)576-5728
E-Mail: reports@adonis.osti.gov
Online ordering: http://www.osti.gov/bridge

Available to the public from
U.S. Department of Commerce
National Technical Information Service
5285 Port Royal Rd
Springfield, VA 22161

Telephone: (800)553-6847
Facsimile: (703)605-6900
E-Mail: orders@ntis.fedworld.gov
Online order: http://www.ntis.gov/help/ordermethods.asp?loc=7-4-0#online

SAND2005-0366
Unlimited Release
Printed April 2005

Final LDRD Report: Design and Fabrication of Advanced Device Structures for Ultra High Efficiency Solid State Lighting

Arthur J. Fischer, Mary H. Crawford
Semiconductor Materials and Device Sciences Department

Daniel D. Koleske, Andrew A. Allerman, Katherine H. A. Bogart
Chemical Processing Science Department

Joel R. Wendt
Photonic Microsystems Technology Department

Randy J. Shul
Microdevice Technologies Department

Sandia National Laboratories
P.O. Box 5800
Albuquerque, New Mexico 87185-0601

Abstract

The goal of this one year LDRD was to improve the overall efficiency of InGaN LEDs by improving the extraction of light from the semiconductor chip. InGaN LEDs are currently the most promising technology for producing high efficiency blue and green semiconductor light emitters. Improving the efficiency of InGaN LEDs will enable a more rapid adoption of semiconductor based lighting. In this LDRD, we proposed to develop photonic structures to improve light extraction from nitride-based light emitting diodes (LEDs). While many advanced device geometries were considered for this work, we focused on the use of a photonic crystal for improved light extraction. Although resonant cavity LEDs and other advanced structures certainly have the potential to improve light extraction, the photonic crystal approach showed the most promise in the early stages of this short program. The photonic crystal (PX)-LED developed here incorporates a two dimensional photonic crystal, or photonic lattice, into a nitride-based LED. The dimensions of the photonic crystal are selected such that there are very few or no optical modes in the plane of the LED ("lateral" modes). This will reduce or eliminate any radiation in the lateral direction so that the majority of the LED radiation will be in vertical modes that escape the semiconductor, which will improve the light-extraction efficiency. PX-LEDs were fabricated using a range of hole diameters and lattice constants and compared to control LEDs without a photonic crystal. The far field patterns from the PX-LEDs were dramatically modified by the presence of the photonic crystal. An increase in LED brightness of 1.75X was observed for light measured into a 40 degree emission cone with a total increase in power of 1.5X for an unencapsulated LED.

Contents

Figures

1. Introduction

Solid state light emitters are poised to revolutionize the lighting industry by producing ultra efficient lighting in compact packages, with more versatile controls, and lifetimes in excess of 50,000 hours. This new lighting technology has the potential to save $100B per year on global electrical energy costs. While standard incandescent light bulbs and fluorescent lamps have luminous efficacies of ~15 lm/W and ~ 80 lm/W, respectively, solid state light emitters have the potential to produce more than 200 lm/W of white light with good color rendering. In order to achieve these efficacies, individual red, green, and blue emitters will need wall plug efficiencies in excess of 50%. For phosphide-based red light emitting diodes (LEDs), wall plug efficiencies as high as 45% [1] have already been reported using advanced chip shaping to improve light extraction. Although one research group has reported a wall plug efficiency in excess of 30% [2] for nitride-based LEDs emitting at 405 nm, such reports are rare and this level of performance has not been realized in a commercial device. Major improvements in both internal and external quantum efficiencies of nitride LEDs are still required in order to realize the full potential of solid state lighting.

Advanced photonic structures offer a means to radically increase the light-extraction efficiency by confining the light emission to readily extracted modes, with some theoretical calculations estimating that extraction efficiencies can be above 90%.[3] Nevertheless, results demonstrated to date have been disappointing due to the difficulty in fabrication and design of such devices. InGaN LED performance can be substantially increased by (1) *enhancing the spontaneous emission efficiency* and/or (2) *enhancing the extraction of light*. High spontaneous emission efficiency is required for high internal quantum efficiencies. The best III-nitride LEDs have only about half the power conversion efficiency compared to state-of-the-art LEDs in the III-phosphide or III-arsenide alloys. A large fraction of the difference in power conversion efficiencies is due to reduced internal quantum efficiencies in the III-nitride LEDs compared to the other material systems. There is considerable on-going work on improving the III-nitride materials by reducing the density of defects and impurities. Photonically engineered structures provide a complementary route to improving the internal quantum efficiency by enhancing the spontaneous emission rate. The lattice constants for the photonic crystals used to fabricate our photonic crystal (PX) LEDs are too large to realize an increase in internal quantum efficiency. Further work will be required to fabricate photonic crystals with a small enough lattice constant to observe a photonically enhanced radiative recombination rate.

The second issue, extraction of light, is a very old problem in LEDs. Light extraction is difficult in an LED due to the large refractive index (n) of typical semiconductors (e.g. around 2.5 for the III-nitrides)—only light within a cone defined by the angle of total internal reflection can escape, which limits light extraction to approximately $1/4n^2$ or less than 5% per surface. One of the largest losses in an InGaN LED is the poor extraction of light from the high-refractive-index semiconductor. The improvements in LED power observed here are due to improvements in light extraction efficiency. A large variety of different optical structures have been employed to enhance the light extraction, with recent results achieving > 55% for an inverted truncated pyramid design used for the phosphide material system[1]. For an RCLED, light extraction is improved by placing the active region inside a Fabry-Perot cavity whose resonance is tuned to the emission wavelength of the LED. The microcavity increases the light emission into vertical modes that are readily extracted. Extraction efficiencies greater than 50% are theoretically possible using an RCLED. For PX-LEDs, a photonic crystal is used to reduce the number of accessible waveguiding modes and direct light into vertical modes with a higher probability of escape from the semiconductor. We start with a standard LED structure and etch a two dimensional array of nanometer scale holes into the nitride-based LED. The required hole diameters will be on the order of 100 – 200 nanometers. This 2D photonic crystal changes the photonic density of states such that the number of lateral waveguiding modes is significantly reduced, which should result in a large improvement in light extraction. For PX-LEDs, theoretical calculations estimate that extraction efficiencies can be above 90%.[3]

For this one year program we quickly down selected to the most promising advanced device implementation which was the photonic crystal LED. For the photonic lattice LED work, we were able to utilize previous InGaN LED epitaxial designs whereas for the RCLED approach, new epitaxial designs were required in addition to developing advanced cleanroom fabrication for RCLEDs. For these reasons, we chose to focus on the development of PX-LEDs for this one year LDRD program. Through the use of a photonic lattice incorporated into an InGaN LED, we were able to show improved performance of 450 nm LEDs.

2. Photonic Crystal Fabrication

A photonic crystal consists of a material with a periodic modulation of the refractive index in one, two, or three dimensions. The refractive index modulation is on a length scale comparable to the wavelength of light in the material, and alters the photonic density of states – i.e., the optical modes available for radiation. Photonic crystals offer new and very powerful methods for controlling light propagation and radiation-matter interactions.[4] In this project, we focused on fabrication of 2-dimensional photonic crystal structures, often referred to as photonic lattices. Photonic lattices were chosen because they offer the promise of significantly increased light extraction, while providing for a practical fabrication approach consisting of mainly planar processing technologies. Thus, one critical part of this effort was the development of an in-house process to fabricate photonic lattices in GaN material. Since optical lithography cannot be used for pattern transfer due to the submicron photonic lattice features, electron beam lithography was used to pattern the photonic lattices. Chlorine based inductively-coupled plasma, reactive ion etching (ICP-RIE) was used to form nanometer scale holes in GaN. GaN is a hard, chemically inert material which is difficult to etch. A considerable amount of developmental work on new masking materials and etch processes was required in order to fabricate photonic lattices in GaN.

2.1. Electron beam lithography

SNL has been applying electron-beam (e-beam) nanolithography to the fabrication of two-dimensional photonic crystal structures in compound semiconductor materials for over ten years. The electron-beam lithography is performed on a JEOL JBX-5FE thermal field emission system featuring a high brightness Gaussian beam with minimum spot size of 5 nm. This system has produced features that resulted in etched, cylindrical holes in GaAs down to 30 nm diameters, which is well below the dimensions that would be required for first-order photonic crystals in GaN materials. Electron beam lithography is also a very flexible technique so that a wide range of geometries (hole array, pitch, and diameter) may be investigated in an efficient manner. The primary drawback of electron-beam lithography is the slow throughput, so that it is primarily useful for research tasks such as exploring a range of lattice parameters rapidly that do not require very large areas. For the PX-LEDs reported here, photonic lattice patterns were written with lattice constants ranging from 270 to 340 nm and hole diameters ranging from 200 to 250 nm. Due to e-beam write time constraints, only small area (170 μm x 170 μm) square devices were patterned.

2.2. GaN etch process development

Since nitride semiconductors are very difficult to etch, particularly when nanoscale photonic lattice dimensions are desired, improvements in the etching process and in the masking materials were required. The etch must be capable of high anisotropies, high aspect ratios, fine features, and good selectivity relative to the mask material. These features can only be obtained with plasma etching techniques. A high-density plasma etching (inductively coupled plasma – ICP) technique was used to etch the holes for our photonic lattices. ICP etchers are highly flexible because they de-couple the plasma generation and acceleration by using two RF sources. This approach also allows for chemical-based etching without compromising the nanostructure geometry (e.g., aspect ratio remains high). This technique is also expected to provide considerably less damage to the III-nitride materials than other dry etching techniques. A very low damage etch might be required to reach the low surface recombination values required to achieve the highest possible efficiency in III-nitride nanostructure LEDs.

Low-damage, high-density plasmas, including ICP, have shown improved etch results for the III-nitrides as compared to RIE. Ion densities often exceeding 5×10^{11} cm^{-3} are produced in the high-density systems, which increases the potential etch rate due to higher ion and neutral reactant flux. ICP is a high-density plasma technique where plasmas are formed in a dielectric vessel encircled by an inductive coil into which rf-power is applied. The electric field produced by the coils in the horizontal plane induces a strong magnetic field in the vertical plane trapping electrons in the center of the chamber and generating a high-density plasma. At low pressures (20 mTorr), the plasma diffuses from the generation region and drifts to the substrate at relatively low ion energy. Thus, ICP etching can produce low damage with high etch rates. Anisotropic profiles are obtained by superimposing an rf-bias on the sample to independently control ion energy. The first ICP etch results for GaN were reported in a $Cl_2/H_2/Ar$ ICP-generated plasma with etch rates as high as 687.5 nm/min. Etch rates increased with increasing dc-bias and etch profiles were highly anisotropic with smooth etch morphologies.[5]

Despite the ability to etch these materials, a significant amount of development work was necessary in order to transfer nanoscale structures into GaN. The primary issue was the development of the masking material required for such small structures. The choice of masking material (resist, oxide, or metal) was optimized to hold up to the Cl-based etching such that the maximum GaN etch depth could be achieved. GaN photonic lattices were etched using a SiO_2 hard masking scheme. SiO_2 films were deposited on the GaN using plasma enhanced chemical vapor deposition (PECVD). Polymethyl methacrylate (PMMA) e-beam resist was spun on the part for use during e-beam patterning. The developed PMMA was used as a mask for a fluorine based RIE etch of the PECVD SiO_2 film. The resulting patterned SiO_2 film was used as a hard mask for the Cl-based ICP etching of GaN. This procedure and other variations of this masking scheme allowed us to fabricate photonic lattices in GaN films.

2.3. Photonic Lattice Characterization

An accurate way of measuring hole diameter, fill factor, and etch depth is critical. The photonic lattices were characterized for dimensional control using an atomic force microscopy (AFM) set-up equipped with a special tip that allows for measurements on the order of ~50nm. An example of an AFM image of a GaN photonic lattice taken in tapping mode is shown in Fig 1. The left image shows a 2 dimensional surface scan of a

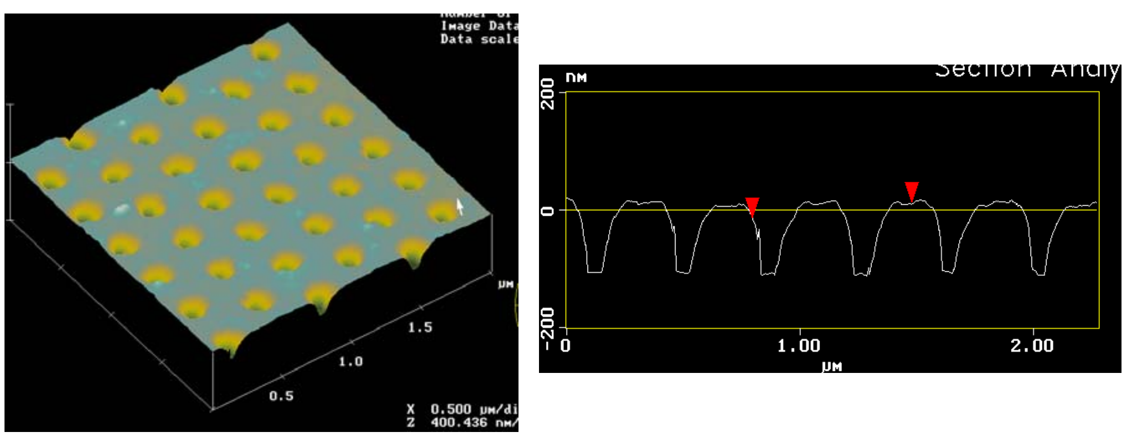

Figure 1. Atomic force microscope data from a photonic lattice fabricated in GaN. The left image shows a 2 dimensional image of triangular lattice with a 347 nm lattice constant. The right image shows a line scan of the data indicating an etch depth of ~ 118 nm..

triangular lattice. The lattice constant for this structure was measured to be ~ 347 nm and the hole diameters are ~ 183 nm at the top. The image on the left shows a cross-sectional line scan of the AFM image. The diameter at the bottom of the hole was measured to be ~ 74 nm and the hole depth is ~ 118 nm. The holes typically do not have straight sidewalls and have a sloped sidewall of about 75 degrees with respect to the GaN surface. This AFM characterization method was used as a non-destructive method of determining the photonic lattice dimensions during PX-LED fabrication.

3. Device Fabrication

InGaN LEDs emitting at 450 nm were fabricated with an incorporated photonic lattice. The photonic lattices were etching into the top GaN layer of the LED using the ICP-RIE etching process described above. LEDs were fabricated with and without photonic lattices in a controlled experiment to determine the effect of the photonic crystal on LED performance.

3.1. PX-LED design

Figure 2 (a) shows the top lit view of a PX LED. The device has an active region area of 170 μm x 170 μm. The outer 10 μm at the edge of the LED mesa is not patterned with a photonic lattice. The center 50 μm x 50 μm is also left unpatterned and contains a dark square where a metal n-contact has been deposited. A shadow of the electrical probe can also be seen in the image. Note that the pattered area appears brighter in the image compared to the areas which were left unpatterned due to the increased light extraction of

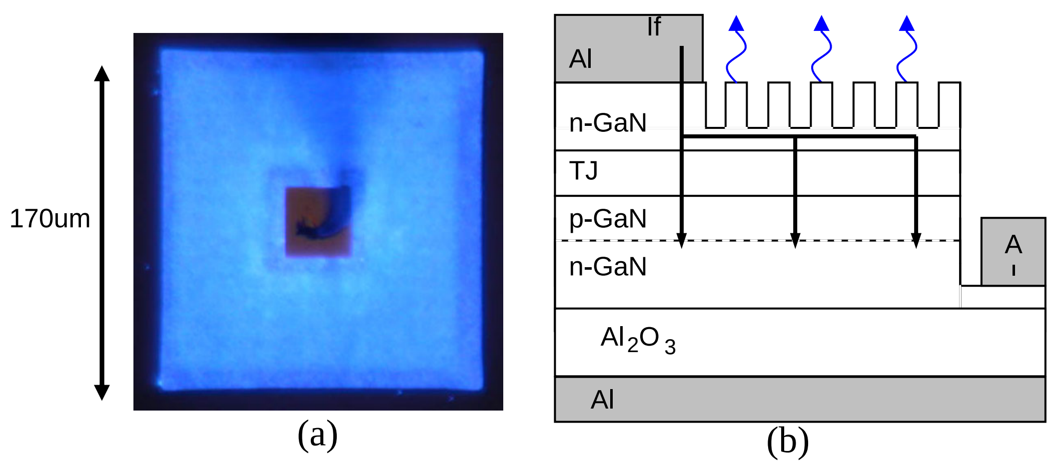

Figure 2. (a) top lit view of the PX-LED and (b) cross-sectional diagram of PX-LED showing the epitaxial structure including a tunnel juntion for hole injection.

the photonic lattice. Figure 2 (b) shows a cross-sectional schematic diagram of the PX-LED. The LEDs were designed as NPN structures with two top side n-contacts. The epitaxial material is grown by metalorganic chemical vapor deposition on sapphire substrates. After the nucleation and buffer layers are grown, n-type GaN is deposited. Next is a multiple quantum well (MQW) active region consisting of $In_xGa_{1-x}N$ wells and GaN barriers emitting at ~ 460 nm. Then ~1500 Å of p-type layers and an InGaN tunnel junction[6] is grown. The structure is completed by ~ 1900 Å of n-GaN. The total epitaxial thickness is ~ 4 μm.

PX-LEDs were fabricated with a range of hole diameters and lattice constants. For the PX-LEDs described in the next section, four different triangular photonic lattices were fabricated labeled PX1, PX2, PX3, and PX4. The PX1 pattern had the smallest dimensions and the PX4 lattice had the largest dimensions. The hole diameter and lattice constants for lattices PX1, PX2, PX3, and PX4 are 200, 220, 235, and 250 nm and 270, 295, 315, and 340 nm, respectively. For these lattice constants and hole diameters no in-plane photonic bandgap is expected. Enhanced extraction is due mainly to Bragg scattering of waveguided modes using higher order diffraction grating. The hole depth was measured by AFM to be ~100 nm for each photonic lattice. The holes were not perfect cylinders and had a sidewall angle of about 75 degrees with respect to the GaN surface. The photonic lattice patterns were etched into the top n-GaN layer of the LED in order to increase extraction of blue light from the LED chip. Wafer level power and radiation pattern measurements were made using unencapsulated LEDs measuring only the emission from the top of the LED wafer.

3.2. PX-LED operating characteristics

The far field radiation pattern for PX-LEDs is dramatically modified compared to control LEDs. The top plot in Fig. 3 shows far field radiation patterns for all four PX-LEDs together with the curve for an unpatterned LED. The far field radiation patterns were measured using a fiber to collect light at specific angular positions above the LED. The inset on the upper left of each plot shows the direction in which the measurement was taken with respect to the photonic lattice pattern. The unpatterned LED in the top plot shows a nearly Lambertian emission pattern with extra emission at +/- 50 degrees due to light escaping from the edge of the LED chip. The intensity for all of the PX-LED is greater then the control LED without the photonic lattice pattern. Note that for PX1 and PX2 light is preferentially scattered into the forward direction. This is a unique feature of PX-LEDs to be able to control the source direction and brightness. This is a very desirable property for many applications where a high brightness is required for illumination. The bottom plot in Fig. 3 shows the far field radiation pattern from pattern PX1 at an angle of f=0 and f= 90 degrees. Note the change in the lobe intensity as the detection plane is rotated by 90 degrees. This is due to the triangular photonic lattice pattern. In fact, a full two-dimensional projected image of the far field radiation (not shown) shows a threefold symmetry as expected from the threefold symmetry of the triangular lattice.

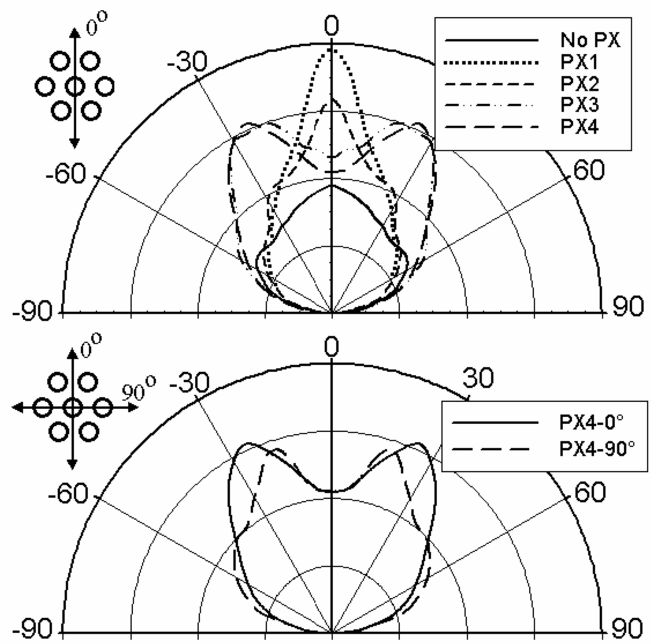

Figure 3. (top) Radiation patterns for PX-LEDs and an unpatterned control LED and (bottom) radiation pattern for PX-4 at ϕ=0 and ϕ= 90 degrees.

The photonic lattice also changed the LED electroluminescence spectrum. Figure 4 shows monochromatic far field radiation patterns for the PX2 pattern and the LED with no photonic lattice. The inset of the figure shows the electroluminescence spectrum for each LED both with emission centered near 460 nm. The plot on the left shows monochromatic far field radiation patterns at three individual wavelengths of

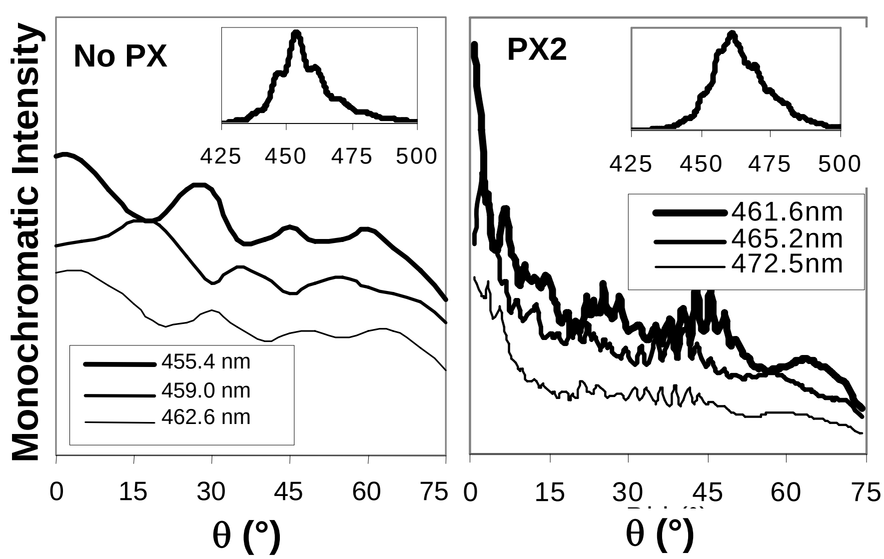

Figure 4. Monochromatic radiation patterns for the (left) no PX and (right) PX2 LEDs. The insets show the electroluminescence spectra.

455.5, 459.0 and 462.6 nm for the LED with no photonic crystal. These curves show only Fabry-Perot interference fringes due to the full 4 μm thickness of the GaN slab. The plot on the right shows monochromatic far field radiation patterns at three similar wavelengths of 461.6, 465.2, and 472.5 nm for the LED with the PX2 photonic lattice pattern. In addition to the broad Fabry-Perot lobes, the LED with a photonic crystal shows additional sharp features due to Bragg scattering of light out of the semiconductor chip.

The output power of each PX-LED was measured as a function of angle and compared to the LED with no photonic crystal. The LEDs were held at an operating current of 33 A/cm2 while measuring the output power as a function of angle. The gain of the photonic crystal LEDs is plotted in fig. 5 as a function of angle for each PX-LED. Gain here is defined as the ratio of output power from a PX-LED to the power from the control LED. The gain plotted here is also integrated from zero degrees to the angle listed, such that the gain at 45 degrees, for example, is the power from the PX-LED into a +/- 45 degree cone divided by the power from the non-PX-LED into the same 45 degree solid angle cone. Thus, the gain at 90 degrees represents the total increase in power for a PX-LED compared to the LED without a photonic crystal. The PX-LED with pattern PX3 shows a 1.5 X increase in total output power compared to the non-patterned control LED. The PX-LED with pattern PX 2 shows a 1.75 X increase in LED brightness into a +/- 40 degree cone as compared to the LED with no photonic lattice. Increased power into a smaller solid angle is desired for many applications where a high brightness source

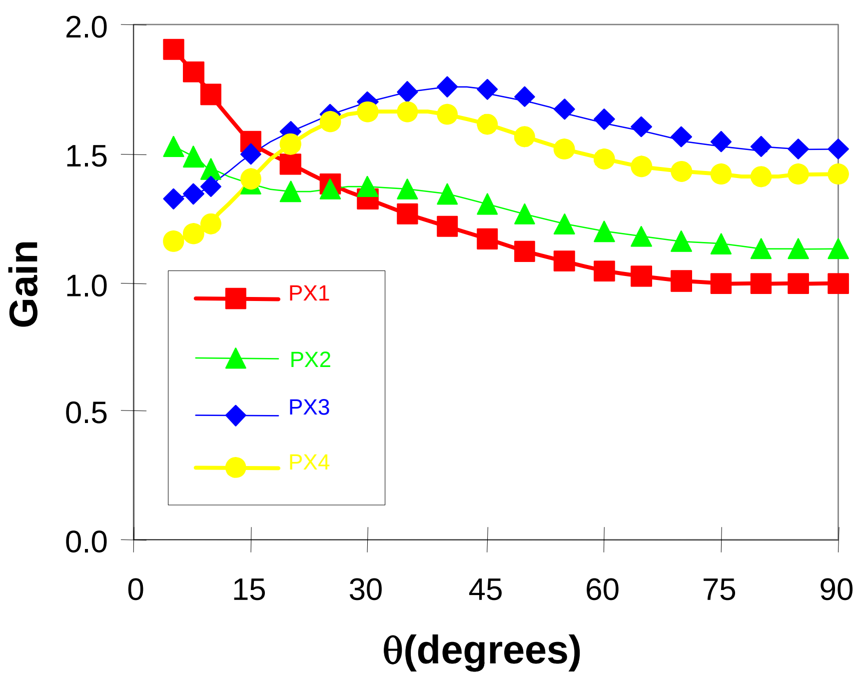

Figure 5. Integrated output power ratio (gain) of the PX-LEDs compared to the LED without a photonic crystal as a function of polar angle.

is required in order to direct illumination without addition optics elements. When incorporated into InGaN LEDs, photonic crystals show promise as a method of increasing the extraction efficiency and thus improving the overall source efficiency.

4. Conclusions

We have developed fabrication methods for etching two dimensional photonic crystals into GaN films. Photonic lattices have been fabricated with lattice constants from 270 to 340 nm with hole diameters ranging from 200 to 250 nm. Atomic force microscopy measurements have shown etch depths on the order of 100 nm, with a sloped sidewall angle of ~ 75 degrees with respect to the GaN surface. LEDs were fabricated with photonic lattices incorporated into the top surface of the LED. These PX-LEDs have a heavily modified far field pattern due to the presence of the photonic lattice. A 1.75 X increase in brightness was observed into a +/- 40 degree cone for one PX-LED. A total output power increase of 1.5 X was measured for a PX-LED compared to a planar control LED. The increased output power is caused by the photonic lattice Bragg scattering light out of the semiconductor chip and improving the overall device efficiency.

Sandia National Laboratory is a multiprogram laboratory operated by Sandia Corporation, for the United States Department of Energy under contract No. DE-AC04-94AL85000. This work was done in collaboration with Mike Krames and Jonathan Wierer from Lumileds Lighting. We would also like to acknowledge the technical support of Kris Fullmer, Mike Banas, Jeff Figiel, and Mike Russell.

5. References

1. M.R. Krames, M. Ochiai-Holcomb, G.E. Höfler, C. Carter-Coman, E.I. Chen, I.-H.Tan, P. Grillot, N.F. Gardner, H.C. Chui, J.-W. Huang, S.A. Stockman, F.A. Kish, M.G. Craford, T.S. Tan, C.P. Kocot, M. Hueschen, J. Posselt, B. Loh, G. Sasser and D. Collins, "High-power truncated-inverted-pyramid $(Al_xGa_{1-x})_{0.5}In_{0.5}P/GaP$ light-emitting diodes exhibiting >50% external quantum efficiency," Appl. Phys. Lett. **75**, 2365 (1999).

2. K. Tadatomo, H. Okagawa, Y. Ohuchi, T. Tsunekawa, H. Kudo, Y. Sudo, M. Kato, and T. Taguchi, "High output power near-ultraviolet and violet light-emitting diodes fabricated on patterned sapphire substrates using metalorganic vapor phase epitaxy," Proceedings of the SPIE **5187,** 243 (2003).

3. S. Fan, P. R. Villeneuve, J. D. Joannopoulos, and E. F. Schubert, "High Extraction Efficiency of Spontaneous Emission from Slabs of Photonic Crystals," Phys. Rev. Lett. **78,** 3294 (1998).

4. J. D. Joannopoulos, R.D. Meade, and J.N. Winn, *Photonic Crystals:Molding the flow of light*, (Princeton University Press, New Jersey, 1995).

5. S.J. Pearton, R.J. Shul, and Fan Ren, "A Review of Dry Etching of GaN and Related Materials," MRS Internet J. Nitride Semicond. Res. 5, 11 (2000).

6. T. Takeuchi, G. Hasnain, S. Corzine, M. Hueschen, R. P. Schneider, Jr., M. Blomqvist, Y.-l. Chang, D. Lefforge, M. R. Krames, L. W. Cook, and S. A. Stockman, "GaN-Based Light Emitting Diodes with Tunnel Junctions," Jpn. J. Appl. Phys. **40**, L861 (2001).

Distribution:

1	MS1427	J. M. Phillips	01100
1	MS1421	J. A. Simmons	01120
1	MS0601	D. L. Barton	01123
2	MS0601	A. J. Fischer	01123
1	MS0601	M. H. Crawford	01123
1	MS0601	R. M. Biefeld	01126
1	MS0601	D. D. Koleske	01126
1	MS0601	A. A. Allerman	01126
1	MS0601	K. H. A. Bogart	01126
1	MS0603	J. R. Wendt	01743
1	MS0603	J. J. Hudgens	01743
1	MS0603	R. J. Shul	01763
1	MS0603	W. K. Shubert	01763
1	MS9018	Central Technical Files	8945-1
2	MS0899	Technical Library	9616
1	MS0188	D. Chavez, LDRD Office	1030